

Optical studies on antimonide superlattice infrared detector material

Linda Hoglund, Alexander Soibel, Cory J. Hill, David Z. Ting, Arezou Khoshakhlagh, Anna Liao, Sam Keo, Michael C. Lee, Jean Nguyen, Jason M. Mumolo, Sarath D. Gunapala

Jet Propulsion Laboratory, California Institute of Technology,
4800 Oak Grove Drive, Pasadena, California, USA 91109-8099

ABSTRACT

In this study the material quality and optical properties of type II InAs/GaSb superlattices are investigated using transmission and photoluminescence (PL) spectroscopy. The influence of the material quality on the intensity of the luminescence and on the electrical properties of the detectors is studied and a good correlation between the photodetector current-voltage (IV) characteristics and the PL intensity is observed. Studies of the temperature dependence of the PL reveal that Shockley-Read-Hall processes are limiting the minority carrier lifetime in both the mid-IR wavelength and the long-IR wavelength detector material studied. These results demonstrate that PL spectroscopy is a valuable tool for optimization of infrared detectors.

Keywords: photoluminescence, heterostructure, infrared, photodetector, superlattice

1. INTRODUCTION

Antimony based type-II superlattices (SL) are considered to be one of the main candidates for next generation high performance infrared (IR) detectors. These SLs typically contain alternating thin layers of InAs and GaSb and the detection is based on type-II interband transitions between the hole energy levels located in the GaSb layers and electron energy levels in the InAs layers. The flexibility of the closely lattice-matched material system of InAs, GaSb and AlSb allows for engineering of the band gap for tailoring of the detection wavelength within the medium-wavelength IR (MWIR, 3-5 μm) region and the long-wavelength IR (LWIR, 8-14 μm) region. It has also enabled new barrier based detector designs [1-4] that are addressing the problems of small bandgap material detectors, such as tunneling across the band gap and dark current related to Shockley-Read-Hall (SRH) processes.

An important parameter for the IR detector performance that reflects the quality of the IR absorbing material is the minority carrier lifetime. This parameter is strongly related to the performance of the device, since carriers excited by the incoming radiation rely on diffusion to the collecting contact layers. If the lifetime is shorter than the diffusion time, the quantum efficiency and detector responsivity are reduced. Even more importantly is that the minority carrier lifetime contains information about defects and traps in the material. These defects and traps act as dark current paths in a detector thus impeding device performance.

Measurement of minority carrier lifetime for small bandgap material has been performed successfully by a few groups using time resolved photoluminescence (PL) and optical modulation response [5]. These measurement are technically challenging, since low excitation power is required to extract a true value of the minority carrier lifetime. The luminescence is relatively weak, compared to corresponding luminescence from semiconductors in the NIR region for which extensive work on time-resolved photoluminescence has been performed [6-8]. An easier method to evaluate the optical quality of the material is by measuring the PL strength. The magnitude of the PL signal indirectly reflects the time constant since it depends on the ratio between the number of charge carriers recombining radiatively compared to the number of non-radiative recombination events.

In this article it will be demonstrated that the intensity of the PL peak serve as a reliable indicator of the detector material quality. PL intensity and the absorption properties of the material are correlated with device parameters, such as quantum efficiency, cut-off wavelength and dark current characteristics. Furthermore, by studying the temperature dependence of the PL of detector material, the limiting processes for the minority carrier lifetime are revealed. These results demonstrate that PL and transmission spectroscopy serve as efficient and valuable tools in the optimization process of

SL detector material. PL is nondestructive and can be employed as an initial tool for wafer characterization to provide critical information not obtained by standard materials analysis techniques such as X-ray diffraction, surface scanning and atomic force microscopy.

2. EXPERIMENTAL DETAILS

2.1 Material growth

SL detector structures were grown in a Veeco Applied-Epi Gen III molecular beam epitaxy chamber equipped with valved cracking sources for the group V Sb₂ and As₂ fluxes, as well as dual In sources for independently varying the growth rates of GaInSb and InAs. Growth was performed on 75 or 50mm diameter Te-doped n-type GaSb (100) substrates.

The energy band diagram of the LW SL detector structures studied (referred to as CBIRD A, B, C and D) is shown in figure 1. This complementary barrier IR detector (CBIRD) design consists of a 300-period (44 Å, 21 Å)-InAs/GaSb absorber SL sandwiched between an 80-period (46 Å, 12 Å)-InAs/AlSb hole-barrier (hB) SL on the left and a 60-period (22 Å, 21 Å)-InAs/GaSb electron-barrier (eB) SL on the right [4]. The hB SL, absorber SL, and eB SL are nominally doped at $n = 1 \times 10^{16} \text{ cm}^{-3}$, $p = 1 \times 10^{16} \text{ cm}^{-3}$, and $p = 1 \times 10^{16} \text{ cm}^{-3}$, respectively. An n-doped InAs_{0.91}Sb_{0.09} layer ($n = 1 \times 10^{18} \text{ cm}^{-3}$) adjacent to the eB SL acts as the bottom contact layer, and the hB SL serves as the top contact layer.

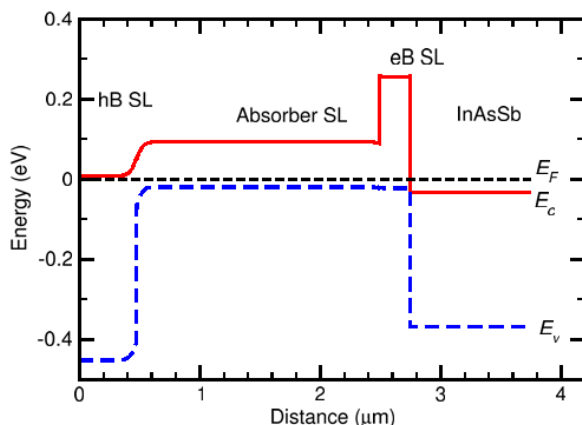


Figure 1. Energy band diagram for a 300-period CBIRD structure.

2.2 Optical measurements

Optical characterization of the SL material consists of two parts: Fourier Transform (FT) transmission measurements as well as FT step scan PL measurements. The measurements are carried out at temperatures between 10 and 298 K using a Thermo-Fisher FT spectrometer, run in fast scan mode for transmission measurements and in step-scan mode during PL tests.

In the PL measurements a 658 nm laser diode is used to excite electrons from the valence band to the conduction band (figure 2 (a)). This generates an additional amount of electrons and holes which relax to the SL band edges. When these carriers recombine, the energy is released by emitting light (PL). The PL peak wavelength serves as a good estimate of the cut-off wavelength of the detector and from the PL intensity and the full-width-half-maximum of the PL spectrum, information about the material quality is obtained. Another important aspect for focal plane array fabrication is the uniformity of the epi-material. Mapping of the PL intensity generates valuable information about the material uniformity across wafer.

The absorption quantum efficiency (QE) of the material and the absorption spectra are extracted from transmission measurements. 10 mm × 5 mm samples are used with the epi-layers removed from half of the sample (figure 2 (b)). The etched part of the sample serves as a reference for the transmission measurements. The measurements are performed in two steps: first the transmission of IR light through the wafer *and* the absorbing material (I, figure 2 (b)) is measured and

then the transmission through the substrate is measured as a reference (I_0 , figure 2(b)). The transmission spectrum is achieved by dividing these two spectra ($T = I/I_0$) and the absorption QE is extracted as $(1-T)$. The reflection coefficient, which is normally included in the expression for absorption QE, can be omitted in this calculation due to the design of the experiment.

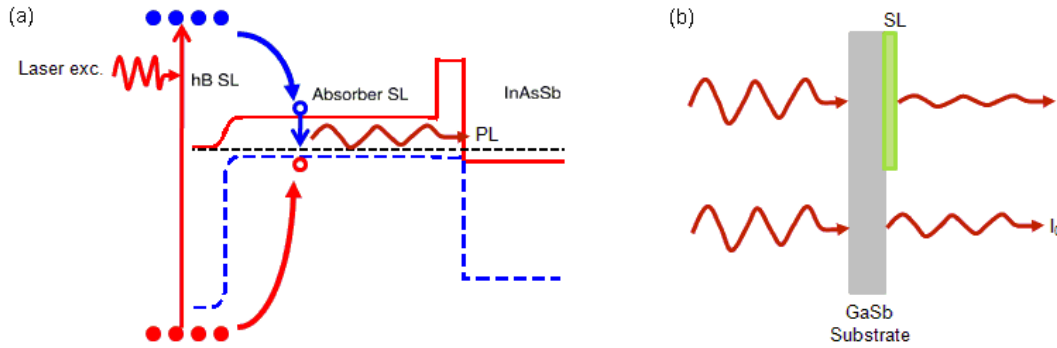


Figure 2. Schematic pictures of the basic principles of (a) PL and (b) transmission measurements

For electrical and optical detector characterization, single element detectors with $200 \mu\text{m} \times 200 \mu\text{m}$ square mesas were fabricated using standard optical lithography, wet chemical etching and evaporation of top and bottom Ti/Pt/Au ohmic contacts. The photodiodes were mounted in a ceramic package using indium and wire-bonded before testing for dark current and responsivity. Dark current measurements were performed in dewar containing liquid nitrogen and the device temperature was controlled by a resistive heater connected to a Lakeshore temperature controller. The photocurrent response was measured using a 1000 K blackbody radiation source and a grating-based monochromator.

3. RESULTS

3.1 Cut-off wavelength and quantum efficiency

Information about the material quality and detector characteristics can be obtained without the need for device fabrication. In figure 3(a) a comparison between the absorption QE, extracted from the transmission measurements as described in section 2, and the external QE is performed. The two spectra are well correlated in terms of spectral distribution; however, the amplitude of the absorption QE is higher than the corresponding external QE. This difference reflects that all photo-generated carriers do not reach the contacts at this specific bias (0.15 V). As the applied bias is increased (figure 3b), the external QE approaches the absorption QE, which serves as an upper limit of the external QE (unless there is gain in the structure). In figure 3a the PL spectrum obtained from the same sample is also plotted, to illustrate the correlation between the cut-off wavelength and the PL peak. From this comparison it can be seen that the PL-peak position serve as a good approximation of the cut-off wavelength of the detector.

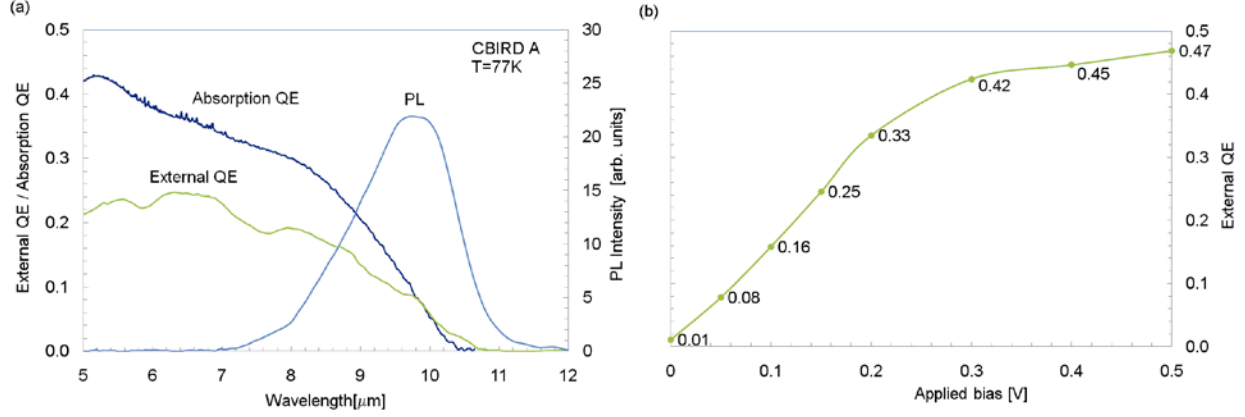


Figure 3. (a) Comparison of the absorption QE and the external QE at an applied bias of 0.15 V (left axis). In the same graph the PL spectrum of the same sample is shown (right axis), illustrating the correlation between the PL-peak and the cut-off wavelength of the detector. (b) Bias dependence of the external quantum efficiency.

3.2 Influence of minority carrier lifetime on PL intensity

Electron-hole pairs generated by laser excitation in the PL measurements are subject to several competing recombination processes, radiative (τ_R) as well as non-radiative (τ_{nR}). The three most common non-radiative recombination processes in semiconductors are SRH recombination, Auger recombination and surface/interface recombination. Compared to bulk material, the influence of Auger recombination in SL material is reduced due to the quantization/strain induced heavy hole – light hole splitting [9,10]. It is consequently assumed that surface recombination and SRH processes dominate the non-radiative lifetime. The lifetimes of these different recombination processes are related to the minority carrier lifetime, τ , as [11]:

$$\frac{1}{\tau} = \frac{1}{\tau_R} + \sum_i \frac{1}{(\tau_{nR})_i}, \quad (1)$$

where each $(\tau_{nR})_i$ is the lifetime associated with a specific non-radiative recombination process. According to equation (1) the smallest of the individual lifetimes will dominate the minority carrier lifetime. The minority carrier lifetime, and therefore the material quality is reflected in PL measurements since the PL intensity is proportional to the ratio between the non-radiative carrier lifetime and the radiative lifetime [11]:

$$PL \propto \frac{\tau_{nR}}{\tau_{nR} + \tau_R} \quad (2)$$

In our experiments, the non-radiative lifetime is smaller than the radiative lifetime and therefore integrated PL intensity reflects the minority carrier lifetime. By comparing PL intensities measured for two wafers with similar design and material structure their respective non-radiative lifetimes, which approximately corresponds to the minority carrier lifetime, are evaluated.

3.3 Correlation between PL and dark current

Traps located in the center of the band gap are not only serving as non-radiative recombination centers during PL, they also serve as efficient excitation paths for electronic transitions between valence and conduction bands, thus increasing the dark current. In this work, the correlation between the PL intensity and the dark current is investigated for three different CBIRD detector samples (CBIRD B-D). Large differences in the PL intensities between these samples are

observed (figure 4a). The highest PL intensity is obtained for CBIRD B, whereas CBIRD C and D have approximately 2 and 20 times lower PL intensities, respectively. A similar trend is observed in the dark current characteristics of these three samples (figure 4b); the lowest dark current is achieved for CBIRD B while the dark current for the CBIRDs C and D is 20 and 290 times larger, respectively (at an applied bias of 0.2V). Some difference in dark current values can be explained by variation of cut-off wavelengths between these devices, nevertheless a significant correlation between a high PL intensity and low dark current is observed. This shows that the PL measurements gives an indication of the material quality and can be used as a predictive tool of the dark current characteristics.

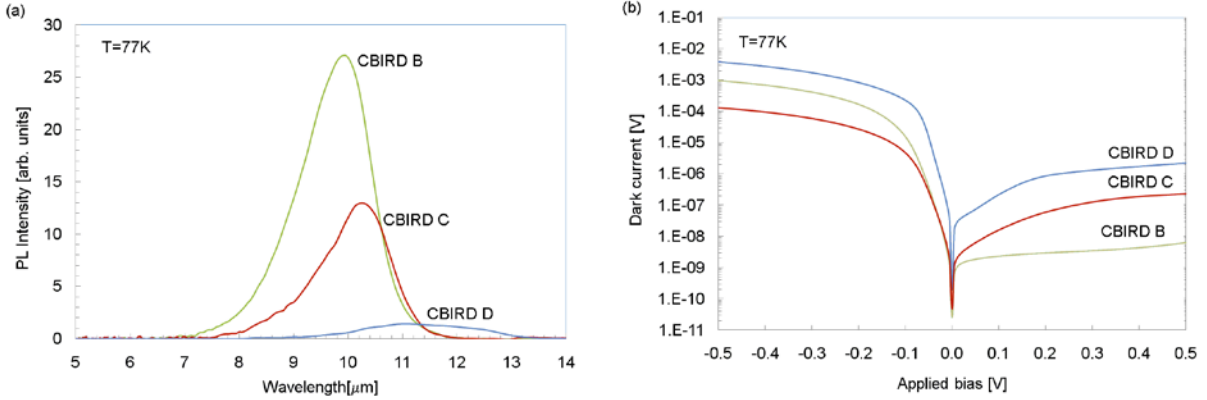


Figure 4. Investigation of the correlation between (a) the peak intensities of the PL spectra and (b) dark current characteristics for three different long wavelength CBIRD detectors.

3.4 Temperature dependence of PL

The correlation between the PL intensity and the minority carrier lifetime (equations 1 and 2) is also used to extract information about which processes limit the minority carrier lifetime of the SL material. When the net carrier lifetime is limited by SRH processes, the PL intensity varies with temperature as [12]:

$$PL \propto \frac{\tau_{SR}}{\tau_{SR} + \tau_R} \propto \frac{1}{T^2} \quad (3)$$

Here, the PL temperature dependences of two different superlattice detectors with cut-off wavelengths at 10 μm and 6.4 μm, respectively, were investigated. With increase of the temperature, redshift of the peak wavelength and a broadening of the PL spectra are observed for both samples (figures 5a and 6a). The temperature dependence of the integrated PL for the LW SL (figure 5b) is well approximated by the $1/T^2$ dependence, which indicates that SRH processes are the limiting factor for the minority carrier lifetime in this material. For the MW sample a good correlation between the integrated PL intensity and the $1/T^2$ dependence is observed at temperatures $> 150K$, however a strong deviation from the $1/T^2$ -dependence is observed at lower temperatures (figure 6b). This deviation at lower temperatures could be attributed to the increase of non-radiative lifetime with decreasing temperature [11] such that the radiative processes become dominant at lower temperatures. Indeed, the PL intensity is almost temperature independent at low T, as is expected when the lifetime is totally dominated by spontaneous emission.

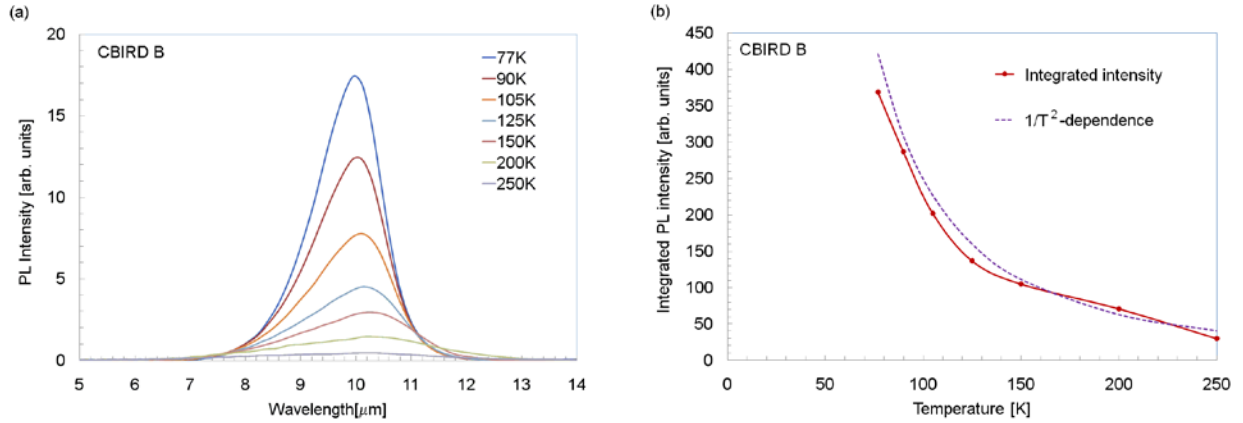


Figure 5. (a) PL spectra for a CBIRD at different temperatures (b) Temperature dependence of the integrated PL intensity compared with a curve showing the theoretical $1/T^2$ dependence associated with SRH processes.

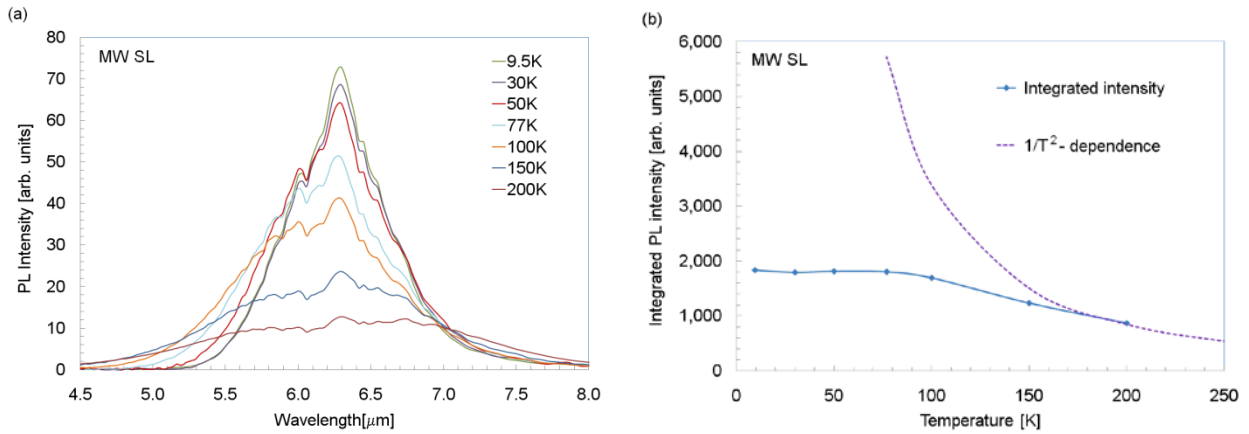


Figure 6. (a) PL spectra for a MW superlattice at different temperatures (b) Temperature dependence of the integrated PL intensity compared with a curve showing the theoretical $1/T^2$ dependence associated with SRH processes.

4. SUMMARY

The material properties of CBIRD detectors have been investigated using two different optical characterization techniques, PL and transmission spectroscopy. The absorption QE, deduced from the transmission measurements, served as a good estimate of the upper limit of the external QE and the PL peak position was shown to correlate well with the detector cut-off wavelength. In a comparison between the PL intensity and the dark current characteristics, a good correlation between a high PL intensity and low dark current was observed, showing that the PL intensity well reflects the material quality. Finally, SRH processes were identified as the limiting factor of the minority carrier lifetime of the CBIRD material studied.

ACKNOWLEDGEMENTS

The research described in this paper was carried out at the Jet Propulsion Laboratory, California Institute of Technology, under a contract with the National Aeronautics and Space Administration. This work was sponsored by the Missile Defense Agency. Copyright 2010 California Institute of Technology. Government sponsorship acknowledged.

REFERENCES

- [1] S. Maimon, G. Wicks, *Appl. Phys. Lett.* 89, 151109 (2006)
- [2] C. L. Canedy, E. H. Aifer, I. Vurgaftman, J. G. Tischler, J. R. Meyer, J. H. Warner, E. M Jackson, *J. Electr. Mat.* 36, 852 (2007)
- [3] P. -Y. Delaunay, B. M. Nguyen, D. Hoffman, E. K. -W. Huang, M. Razeghi, *IEEE J. Quant. Electr.* 45,157 (2009)
- [4] D. Z. -Y. Ting, C. J. Hill, A. Soibel, S. A. Keo, J. M. Mumolo, J. Nguyen, S. D. Gunapala, *Appl. Phys. Lett.* 95, 023508 (2009)
- [5] D. Donetsky, S. P. Svensson, L. E. Vorobjev, G. Belenky, *Appl. Phys. Lett.* 95, 212104 (2009)
- [6] A. Fiore, P. Borri, W. Langbein, J. M. Hvam, U. Oesterle, R. Houdre, R. P. Stanley, M. Ilegems, *Appl. Phys. Lett.* 76, 3430 (2000)
- [7] S. Marcinkevicius, U. Olin, J. Wallin, K. Streubel, G. Landgren, *Appl. Phys. Lett.* 65, 2057 (1994)
- [8] R. Heitz, I. Mukhametzanov, H. Born, M. Grundmann, A. Hoffmann, A. Madhukar, D. Bimberg, *Physica B* 272, 8 (1999)
- [9] C. H. Grein, P. M. Young, M. E. Flatte, H. Ehrenreich, *J. Appl. Phys.* 78, 7143 (1995)
- [10] D. Z.-Y. Ting, S. V. Bandara, C. J. Hill, S. D. Gunapala, Y.-C. Chang, H. C. Liu, C. Y. Song, A. Soibel, J. Mumolo, J. Nguyen, J. K. Liu, S. A. Keo, S. B. Rafol, and E. R. Blazewski, *Proc. of SPIE*, Vol. 7298, 729805-1 (2009)
- [11] R. K. Ahrenkiel, [*Semiconductors and Semimetals*, Vol 39], Academic Press, Inc., San Diego, 40-150 (1993)
- [12] C. L. Canedy, W. W. Bewley, C. S. Kim, M. Kim, I. Vurgaftman, J. R. Meyer, *J. of Appl. Phys.* 94, 1347 (2003)